

Magnetic-Based Biocomposites in Dye Adsorption



Adewale Adewuyi

Abstract Adsorption is an important method used in the removal of dyes from the water system. The application of magnetic-based biocomposite as an adsorbent in the adsorption process to remove dyes from water is a possible technique in wastewater purification. This chapter focuses on the production and application of magnetic-based biocomposite in the removal of dyes from water. It was evident that magnetic-based biocomposites are potential adsorbent for the removal of dyes from water. However, there is scanty information available on the use of magnetic-based biocomposites on a large scale, as most studies reported were on a laboratory scale. Despite the promise of high efficiency exhibited by magnetic-based biocomposites towards dyes in water, there is a need to evaluate their economic viability and prospects on a large-scale application.

Keywords Adsorption · Biocomposites · Desorption · Dye · Magnetite · Wastewater

1 Introduction

Pollution of water resources by organic molecules such as dyes is a serious global challenge. Many dyes are produced yearly, which end up in the environment during or after use. Dyes have found application in several industries such as paper, leather, textile, cosmetic, food and plastics [25]. Most dyes are toxic and carcinogenic [39], which can cause havoc to health and, when they get into the environment, may cause long-term adverse effect on plants, animals and human beings. About two-thirds of over 100,000 commercially known dyes are consumed by textile industries, which generate a large volume of coloured wastewater [74]. The colour produced by the dyes in water is highly discernible and inadmissible due to its ability to prevent reoxygenation in water. Furthermore, it disrupts microorganism activities in aquatic

A. Adewuyi (✉)

Department of Chemical Sciences, Faculty of Natural Sciences, Redeemer's University, Osun State, Ede, Nigeria

e-mail: walexy62@yahoo.com

system because it inhibits the penetration of sunlight [79]. Most dyes have complex chemical structures, soluble in aqueous systems and persistent when they get into the environment. When in the environment, they are often exposed to environmental factors that may degrade them to form intermediates that are more toxic than their original forms. Therefore, it is crucial to understand the fate of these dyes when they get into the environment. Moreover, the need to develop efficient techniques for their complete removal in water cannot be overemphasized. Although some of the dyes have been banned in many countries, they are still widely used in other countries [49]. Among the numerous dyes known, the azo dye remains the largest synthetic dyes class with a wide application [49]. It is aromatic, and because of the possibility of reductive cleavage taking place at the azo linkages that may lead to the formation of amines, azo dyes are considered toxic. The diazo dye groups are also common and are toxic. An example of this is congo red dye which may be prepared by coupling tetrazotized benzidine with two molecules of naphthionic acid. Previous studies have reported dyes in surface and underground water system, as presented in Table 1. When the dyes get into the water bodies, they cause an increase in the levels of biochemical oxygen demand (BOD) and chemical oxygen demand (COD); the main concern is in the non-biodegradability of some of the dyes [47].

Although dyes may be grouped as natural or synthetic, their classification may also be based on colour, chemical structure, particle charge in solution and application. Natural dyes are sourced from plant and animals; however, as scientific knowledge advanced, the properties of natural dyes were improved by way of chemical synthesis, which led to synthetic dyes. Over time, synthetic dyes have gradually replaced their natural counterparts due to improved performance and aesthetics. Synthetic dyes may be ionic or non-ionic, with examples such as direct, acid, vat, basic, dispersed and reactive dyes. The reactive, direct, acid and basic dyes are

Table 1 Reported presence of dye in environmental water system

Source	Dye type	Country	References
Cristais river	Disperse azo, disperse Blue 373, disperse orange 37 and disperse violet 93	Brazil	[10]
Ribeirão das Cruzes river	Basic red 51	Brazil	[15]
River water	Disperse dyes	China	[82]
Pearl river delta	<i>N</i> -nitrosamines	China	[12]
Raw river water and drinking water treatment plant	<i>p</i> -aminophenol	Brazil	[19]
Cristais river	Disperse blue 373, disperse violet 93 and disperse orange 37	Brazil	[18]
Ripoll river	Textile dye	Spain	[14]
Archaeological sites	Natural dyes	China	[34]
River water and sediment	Azo dyes	Japan	[27]
Khniss and Hamdoun rivers	Disperse dyes	Tunisia	[40]

mostly water-soluble [36], making it difficult to remove them from water [26]. They persist in the environment; a recent investigation has shown that when azo dyes are used, about 15–50% remain in water without binding to fabric, making azo dyes a significant contributor of dye to the environment [31]. The presence of these dyes in the environment is undesirable; therefore, it is important to remove them from water systems before they get into the environment. Approaches reported as potential methods of removal included oxidation, membrane separation, advanced oxidation, electrochemical process, flocculation, ion exchange and adsorption.

Varieties of methods reported for the removal of dyes from water are known to rely on chemical, physical or biological techniques [8] in their operations. The chemical technique has the advantage of being effective at both high and low concentration of dye, however, it leads to the production of unwanted chemical deposition of sludge as secondary pollutants, which require additional cost for removal and sometimes may be far more problematic than the dye to be removed. Apart from this, the process requires a large number of chemical reagents and energy consumption [65, 84]. The biological technique is simple and requires the use of microorganisms to decolourize the dye contaminated water system; however, the process needs to be under specific conditions such as controlled process pH, temperature and nutrition, which may make it complex and expensive to start up or maintain [46]. Adsorption and membrane separation are typical examples of the physical techniques used [56]. Since the use of a membrane is limited with poor reusability, adsorption is a better process in terms of physical technique. Most dyes are resistant to degradation due to their complex chemical structure. Therefore, adsorption remains outstanding among the methods developed over time for removing dyes in the water system. Apart from being efficient, adsorption is cheap, reliable and can be easily set up. The use of adsorption is sustainable, and environmentally friendly. Since the adsorbents used can be regenerated and reused as appropriate, adsorption is considered a viable option for removing dyes from water.

Generally, an adsorbent is considered suitable for removing dyes from water system when its effective surface area for the sorption process is large with high adsorption capacity, excellent regeneration capacity and outstanding performance at a wide pH range. Several adsorbents have been reported in time past to remove dyes in the water system, as shown in Table 2. Despite the high adsorption capacities exhibited by some of these adsorbents, they still suffer from certain limitations that border on effective regeneration for long-term use and separation from the water system after the sorption process. Recent studies have shown that the use of magnetic-based biocomposite can help circumvent these limitations. In line with this, this chapter focuses on the use of magnetic-based biocomposites to remove dyes in solution.

2 Adsorption as a Process for Dye Removal

Adsorption as a process in dye removal from solution may be described as the decolourization of water contaminated with dye by attachment of dye molecules

Table 2 Selected adsorbents previously reported for the removal of named dyes in solution

Adsorbent	Dye type	Adsorption capacity (mg g ⁻¹)	References
Mesoporous zeolite	Crystal violet	1217	[9]
Montmorillonite/graphene oxide composite	Crystal violet	746	[48]
Montmorillonite/graphene oxide composite	Methylene blue	641	[76]
Kaolin-based mesoporous silica	Methylene blue	653	[33]
Mesoporous zeolite	Methylene blue	548	[9]
Cellulose/clay composite hydrogel	Methylene blue	277	[63]
Smectite rich natural clays	Basic yellow 28	77	[11]
Chitosan sponge	Rose Bengal	602	[61]
Chitosan/surfactant composite	Orange G	1452	[80]
Chitosan/polyvinyl alcohol/zeolite	Methyl orange	153	[24]
Polyurethane/chitosan foam	Food red 17	267	[16]

to a solid surface by chemical or physical interaction [44]. The solid surface is known as adsorbent, while the dye adsorbed from solution is known as adsorbate. If the interaction between the adsorbate and the adsorbent is physical, the adsorption process is referred to as physisorption. In contrast, when the interaction forces are due to chemical bonding, it is referred to as chemisorption [73]. The removal of adsorbate from the surface of the adsorbent is known as desorption which is the reverse of adsorption. In the case of physisorption, the interaction forces are weak, such as Van der-Waals forces. The process is easily reversed in physisorption resulting in desorption due to the weak forces of interaction, but desorption is difficult in the case of chemisorption.

It is crucial to determine the amount of adsorbate an adsorbent can accumulate, which helps understand its adsorption capacity, which may be calculated from adsorption isotherm. Since dyes are not easily broken down, they can be removed from the solution via adsorption. The adsorbent should have a short removal time, high uptake kinetic and good surface character for removal [6]. The adsorption capacity is the mass of adsorbate (dye) adsorbed per unit mass of adsorbent (magnetic-based biocomposite). Lots of isotherm models have been developed to describe the adsorption process; such isotherm models include Langmuir, Freundlich, Temkin, Hill, etc.

The Langmuir isotherm model is a model that assumes that the molecules adsorbed on the surface of the adsorbent form a monolayer, and each adsorbate on the surface of the adsorbent has the same adsorption activation energy; the model can be expressed as [59].

$$\frac{C_e}{q_e} = \frac{1}{Q_o} C_e + \frac{1}{Q_o K_L} \quad (1)$$

where C_e (mg L^{-1}) is the equilibrium amount of adsorbate, q_e (mg g^{-1}) is the amount of adsorbate removed at equilibrium, Q_o (mg g^{-1}) is the maximum monolayer coverage capacity and K_L (L mg^{-1}) represents the Langmuir isotherm constant. To better understand the Langmuir isotherm model, it is important to determine the value of R_L , which is an essential feature of the Langmuir isotherm that can be expressed as:

$$R_L = \frac{1}{1 + K_L C_o} \quad (2)$$

It has been reported that when $R_L > 1$, the sorption process is unfavourable, when $R_L = 1$, the sorption is considered linear when $0 < R_L < 1$, the process is favourable, and when $R_L = 0$, the process is taken to be irreversible [2, 3].

The Hill model is different from Langmuir; unlike the Langmuir model, which assumes that each adsorption site on the adsorbent can only accept one mole, the Hill model was developed on the fact that each adsorption site can accept n molecules of the adsorbate, which can be expressed as [6]

$$Q = \frac{nM_m}{1 + \left(\frac{C_{1/2}}{C}\right)^n} \quad (3)$$

Q is the equilibrium adsorption capacity (mg g^{-1}), n represents the number of molecules connected at each adsorption site, $C_{1/2}$ is the adsorbate concentration at half-saturation (mg g^{-1}) and where N_m represents the number of occupied adsorption sites.

Adsorption studies have also been subjected to the Freundlich isotherm model, which may be expressed as:

$$q_e = K_f C_e^n \quad (4)$$

where the equilibrium concentration of the adsorbate is represented as C_e (mg L^{-1}), K_f (mg g^{-1}) represents the Freundlich isotherm constant, q_e (mg g^{-1}) is the amount of the adsorbate adsorbed at equilibrium on the adsorbent and the adsorption intensity is represented as n . The Freundlich model is a multilayer sorption which describes the sorption process on a heterogeneous surface as an exponential distribution of active sites and their energies. It is also important to check the effect of certain parameters on the sorption capacity of an adsorbent; such parameters include the effect of temperature, pH, adsorbate concentration, adsorbent particles and adsorbent dose. Despite the several adsorbents known, the use of magnetic-based biocomposites in removing dye from solution remains outstanding because of the ease of separation after the adsorption of dye by the simple application of magnet [71].

Different types of adsorption kinetic and diffusion models have been proposed, among which pseudo-first-order, pseudo-second-order, intra-particle diffusion and Elovich models are common. The pseudo-first-order model may be represented as:

$$\log(q_e - q_t) = \log q_e - \frac{K_1}{2.303}t \quad (5)$$

where q_e (mg g⁻¹) is the equilibrium amount of dye ions, q_t (mg g⁻¹) represents the dye ions adsorbed at a specific time, k_1 (min⁻¹) stands for the rate constant for pseudo-first-order adsorption and t is the time (min). From this expression, k_1 and q_e can be determined from the plot of $\log(q_e - q_t)$ against t .

The pseudo-second-order model may be described as:

$$\frac{t}{q_t} = \frac{1}{k_2 q_e^2} + \frac{1}{q_e}t \quad (6)$$

where q_e (mg g⁻¹) is the equilibrium amount of dye ion, q_t (mg g⁻¹) is the amount of dye ion adsorbed at a specific time, and k_2 (g mg⁻¹ min⁻¹) represents the rate constant for the pseudo-second-order model. The value of q_e and k_2 may be determined from the various plots as described in Table 3.

The sorption may be further described using the intra-particle diffusion model, as expressed:

$$q_t = k_{id}t^{0.5} + C \quad (7)$$

where the k_{id} is the diffusion constant (mg g⁻¹ min^{1/2}) while C (mg g⁻¹) represents a constant that shows the layer thickness. The parameters can be determined from the plot of q_t against $t^{1/2}$. C is the value of the intercept, which is related to the boundary layer thickness. The larger the intercept value from the plot, the greater the boundary effect will be [28]. The data generated from the sorption process can also be subjected to the Elovich model, which can be linearized as:

$$q_t = \frac{1}{\beta} \ln(\alpha\beta) + \frac{1}{\beta} \text{Int} \quad (8)$$

Table 3 Forms of pseudo-second-order expression from which q_e and k_2 may be determined

Type	Form	Graph plot	Parameters
1	$\frac{t}{q} = \frac{1}{k_2 q_e^2} + \frac{1}{q_e}t$	$\frac{t}{q_t}$ VS. t	$q_e = \frac{1}{\text{Slope}}$; $K_2 = \frac{\text{Slope}^2}{\text{Intercept}}$; $h = \frac{1}{\text{Intercept}}$
2	$\frac{1}{q} = \left(\frac{1}{k_2 q_e^2}\right) \frac{1}{t} + \frac{1}{q_e}$	$\frac{1}{q_t}$ VS. $\frac{1}{t}$	$q_e = \frac{1}{\text{Intercept}}$; $K_2 = \frac{\text{Intercept}^2}{\text{Slope}}$; $R = \frac{1}{\text{Slope}}$
3	$\frac{1}{t} = \frac{K_2 q_e^2}{q} - \frac{K_2 q_e^2}{q_e}$	$\frac{1}{t}$ VS. $\frac{1}{q_t}$	$q_e = \frac{-\text{Slope}}{\text{Intercept}}$; $K_2 = \frac{\text{Intercept}^2}{\text{Slope}}$; $R = \text{Slope}$
4	$\frac{q}{t} = K_2 q_e^2 - \frac{K_2 q_e^2 \cdot q}{q_e}$	$\frac{q_t}{t}$ VS. q_t	$q_e = \frac{-\text{Intercept}}{\text{Slope}}$; $K_2 = \frac{\text{Slope}^2}{\text{Intercept}}$; $R = \text{Intercept}$

where α is the rate ($\text{mg g}^{-1} \text{min}^{-1}$), and β is the magnitude of coverage (g mg^{-1}) that are determined from the intercept and slope of the plot of q_t vs Int.

3 Preparation of Magnetic-Based Biocomposite

Preparation of magnetic-based biocomposite may be achieved using several methods which cover chemical vapour deposition, co-precipitation, solvothermal, microwave-assisted, hydrothermal, photolysis, sonochemical, sol-gel, laser pyrolysis, annealing, microemulsion, electrodeposition and thermal deposition [17, 32, 43, 45, 50, 67, 68, 70]. Several starting materials as feedstock have been reported in the synthesis of magnetic-based biocomposites; some of this includes biomass such as agricultural products and wastes containing lignin, cellulose and hemicellulose with polyphenolic functional groups which bind with dye via different mechanisms. Recently, the biomasses are converted to carbon nanoparticles with the inclusion of magnetic metal oxide to impose magnetic properties on the composite. Biocomposites produced this way have improved particle size and shape distribution, crystallinity, structure, pore size, surface area and stability. A large number of magnetic nanomaterials have been prepared and used in the removal of dyes from wastewater [54]; some of these include the use of metallic nanomaterials (nano- Fe_2O_4 , nano- MnFe_2O_4 , nano- ZnO , nano- TiO_2 , etc.), carbonaceous nanomaterials (graphene, carbon nanotubes, etc.) and bionanomaterials (nanochitosan, nanocellulose, etc.).

A study by Wang et al. [62] reported the preparation of a magnetic composite adsorbent using graphene multi-walled carbon nanotube for the removal of methylene blue from solution. The composite exhibited an adsorption capacity of 65.79 mg g^{-1} with good regeneration capacity. Another study [13] made use of β -Cyclodextrin and carbon in the preparation of a magnetic composite to remove methylene blue from the solution. The magnetic properties exhibited by the biocomposites may be determined by applying an external magnetic field to them. The orientation of magnetic moment displayed by the biocomposites helps identify the magnetism they possess, which may be ferromagnetism, diamagnetism, ferrimagnetism, ferromagnetism or anti-ferromagnetism [5]. The magnetism exhibited by magnetic biocomposites can be attributed to their high surface-area-to-volume ratio [57]. The property varies with the size and shape of the composite. The specific magnetic property displayed by a biocomposite is mainly determined by its composition, which depends on the presence or absence of unpaired valence electrons located on the metal atoms or ions found in the composite [83]. Magnetic metal oxide biocomposites have shown high adsorption capacity towards dye contaminated water. They were earlier prepared by co-precipitation, and have been found to be environmentally friendly and cost-effective [4]. Their particle size, porous structure and outstanding magnetic properties make their recovery by magnetic separation technology after adsorption or regeneration easy. This ease of recovery gives the use of magnetic-based biocomposite an advantage over powder adsorbents in the removal of dyes from wastewater.

4 Magnetic-Based Biocomposite as Dye Adsorbent

One of the major advantages of using magnetic-based biocomposites is the short treatment time. A large volume of dye contaminated water can be cleaned within a short time, and process recovery is superb. Since synthetic magnetic materials may be expensive, attention has shifted towards the use of bio-based materials in order to obtain low-cost magnetic material, which has led to the preparation of magnetic-based biocomposite. A previous study [42] revealed xanthan gum grafted poly (acrylic acid)-based Fe_3O_4 hydrogel nanocomposite as a suitable material for the sorption of methyl violet with an adsorption capacity of 642 mg g^{-1} . A reported study [41] further showed the synthesis and application of gum Ghatti-based iron oxide hydrogel nanocomposite as remediation means for methylene blue contaminated water; the biocomposite exhibited a maximum adsorption capacity of 671.14 mg g^{-1} . Recently, the preparation of magnetic hydrogel biocomposite via free radical polymerization method for the sorption of methylene blue was reported [38]. The hydrogel biocomposite exhibited a high maximum adsorption capacity ($1109.55 \text{ mg g}^{-1}$) in an adsorption process that may be described spontaneous and endothermic in nature. A study [37] revealed the synthesis of magnetic composite based on saponite clays with magnetite (2–7 wt%) content; characterization of the composite showed a more developed mesoporosity and microporosity when compared to saponite clay with a capacity to remove malachite green, congo red and indigo carmine from solution.

In order to reduce the production cost of magnetic-based biocomposite, it is preferable to use waste materials as feedstock. Industrial and agricultural waste materials could be used. They can be used as a low-cost adsorbent; however, the introduction of magnetic properties helps in improving the performance of the resulting biocomposite. The agricultural waste may include leaves, fruits peels, seeds and fibres. This may also include waste materials like sawdust, stem bark and wood shavings which may serve as cheap sources of lignin, cellulose and hemicellulose required for the biocomposite preparation. An example of this is the preparation of magnetically modified spent coffee ground for the sorption of safranin O, amido black 10B, crystal violet, bismarck brown Y, congo red, acridine orange and malachite green [50]. Organic dyes have also been removed from the solution using ferrofluid-modified peanut husks with encouraging adsorption capacity in a process that may be described by Langmuir isotherm [51]. Biodegradable magnetic-based adsorbent has also been prepared mainly from glutamic acid and chitosan [75]; the resulting glutamic acid-modified chitosan magnetic biocomposite microspheres were used for the removal of methylene blue, light yellow and crystal violet from solution with an adsorption capacity which was as high as 375.4 mg g^{-1} . The impressive adsorption capacity exhibited by the glutamic acid-modified chitosan magnetic biocomposite was attributed to its high surface area. The dyes were further desorbed from the composite, which was regenerated using simple regenerating agents (HCl and NaOH). Novel magnetic carbon-iron oxide nanocomposite was reported [58] for the removal of crystal violet dye from solution; the sorption capacity was determined to be 113.31 mg g^{-1} at an optimal condition in a process that obeys Langmuir

isotherm. Recently, a safe and cost-effective method was developed for the treatment of dye contaminated water system [53]. It involved the synthesis of magnetic nanocomposite-based polyacrylic acid cross-linked with magnetic 3D cross-linkers and carboxylated cellulose, as described in Fig. 1. During the synthesis, acrylic functionalized Fe_3O_4 particles were covalently linked to the polymer chains to introduce the magnetic properties; the inclusion of highly dispersed carboxylated cellulose nanocrystals reduced the gel-like properties of the nanocomposite. The composite was found efficient towards the removal of cationic dyes from water with a maximum adsorption capacity of 332 mg g^{-1} . Different magnetic-based composites previously reported in the past and their adsorption capacities are presented in Table 4.

The use of gum xanthan-grafted-polyacrylic acid and Fe_3O_4 magnetic nanoparticles based nanocomposite hydrogel have also been documented for the removal of methyl violet from aqueous solution [41]. The proposed mechanism for the synthesis is as shown in Fig. 2. The synthesized Fe_3O_4 magnetic nanoparticles based nanocomposite hydrogel exhibited a 99% removal of methyl violet from solution with an adsorption capacity of 642 mg g^{-1} , which may be described by a pseudo-second-order kinetics model. Similarly, a study [60] recently reported a new hydrogel nanocomposite based on chitosan-grafted-polyacrylic acid/oxidized electrospun carbon nanofibres; an illustration of the preparation steps is shown in Fig. 3. The hydrogel composite exhibited a high adsorption capacity of 1095 mg g^{-1} towards methylene blue and good regeneration capacity with promising potentials as a prospective low-cost adsorbent for treating wastewater.

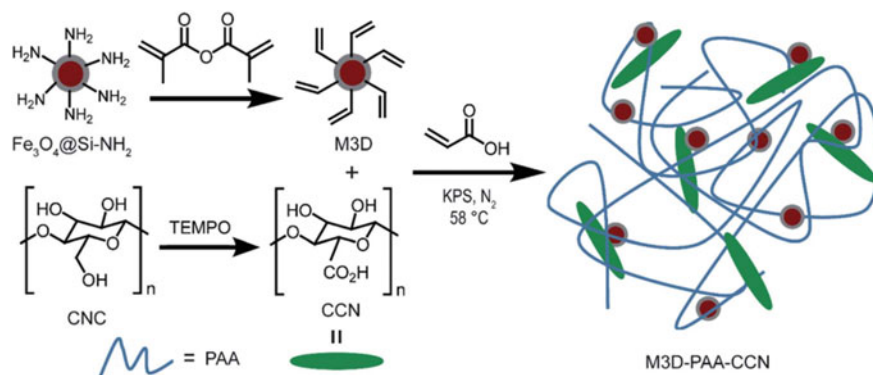


Fig. 1 Schematic illustration of the synthesis of M3D-PAA-CCN nanocomposite [53]. PAA = Polyacrylic acid, CNC = Carboxylated cellulose nanocrystals, CCN = carboxylated cellulose nanocrystals, M3D-PAA-CCN = Magnetic 3D-polyacrylic acid-carboxylated cellulose nanocrystals

Table 4 Previously reported magnetic-based composites for dye removal, their adsorption isotherm, kinetic models and capacities

Adsorbent	Dye	Isotherm model	Kinetic model	Adsorption capacity (mg g ⁻¹)	References
Magnetic Fe ₃ O ₄ @ GPTMS and Lys	Orange I	Langmuir	Pseudo 2nd order	83	[81]
Magnetic Fe ₃ O ₄ @ GPTMS and Lys	Acid red 18	Langmuir	Pseudo 2nd order	71	[81]
Magnetic Fe ₃ O ₄ @ GPTMS and Lys	Azure I	Langmuir	Pseudo 2nd order	190	[81]
Magnetic Fe ₃ O ₄ @ GPTMS and Lys	Methyl blue	Langmuir	Pseudo 2nd order	185	[81]
Graphene-Fe ₃ O ₄ nanocomposite	Pararosaniline	Langmuir	Pseudo 2nd order	198.23	[66]
Magnetic Fe ₃ O ₄ @ graphene	Congo red	Langmuir	Pseudo 2nd order	33.06	[77]
Magnetic graphene oxide	orange G	Langmuir	Pseudo 2nd order	20.85	[20]
Magnetic Zn Fe ₂ O ₄ nanoparticles	Acid red 88	Langmuir	Pseudo 2nd order	111.1	[30]
Chitosan supported CNT-MNPs	Acid red 18	Langmuir	Redlich–Peterson	809.9	[64]
EDTAD modified magnetic chitosan	Methylene blue	Sipss	Pseudo 2nd order	113.26	[69]
Fe ₃ O ₄ /CeO ₂ (Fe/Ce) nanocomposite	Acid black 210	Langmuir	Pseudo 2nd order	90.50	[23]
M3D-PAA-CCN	Methylene blue	Langmuir	Pseudo 2nd order	332	[53]
Magnetic hydrogel nanocomposite	Methylene blue	Langmuir	Pseudo 2nd order	1081.60	[38]
Magnetic graphene oxide composite	Acid blue 113	Langmuir	Pseudo 2nd order	32.2	[78]
Fe ₃ O ₄ /AC/CD/Alg	Methylene blue	Langmuir	Pseudo 2nd order	10.63	[72]
S-doped Fe ₂ O ₃ /C nanocomposite	Congo red	Langmuir	Pseudo 1st order	270.20	[29]
Rice bran-based magnetic composite	Reactive blue 4	Langmuir	Pseudo 2nd order	218.82	[35]
Rice bran-based magnetic composite	Crystal violet	Langmuir	Pseudo 2nd order	159.24	[35]
Strontium ferrite-bentonite-composite	Eriochrome black T	Freundlich	Pseudo 2nd order	329.61	[21]

(continued)

Table 4 (continued)

Adsorbent	Dye	Isotherm model	Kinetic model	Adsorption capacity (mg g^{-1})	References
Strontium ferrite-bentonite-composite	Methyl orange	Freundlich	Pseudo 2nd order	219.56	[21]

Fe₃O₄/AC/CD/Alg = magnetic iron oxide (Fe₃O₄)/activated charcoal (AC)/ β -cyclodextrin (CD)/sodium alginate (Alg) polymer nanocomposite, M3D-PAA-CCN = Magnetic 3D-polyacrylic acid-carboxylated cellulose nanocrystals, GPTMS = toxic 3-glycidoxypropyltrimethoxysilane, Lys = Lysine, MNPs = magnetic nanoparticles

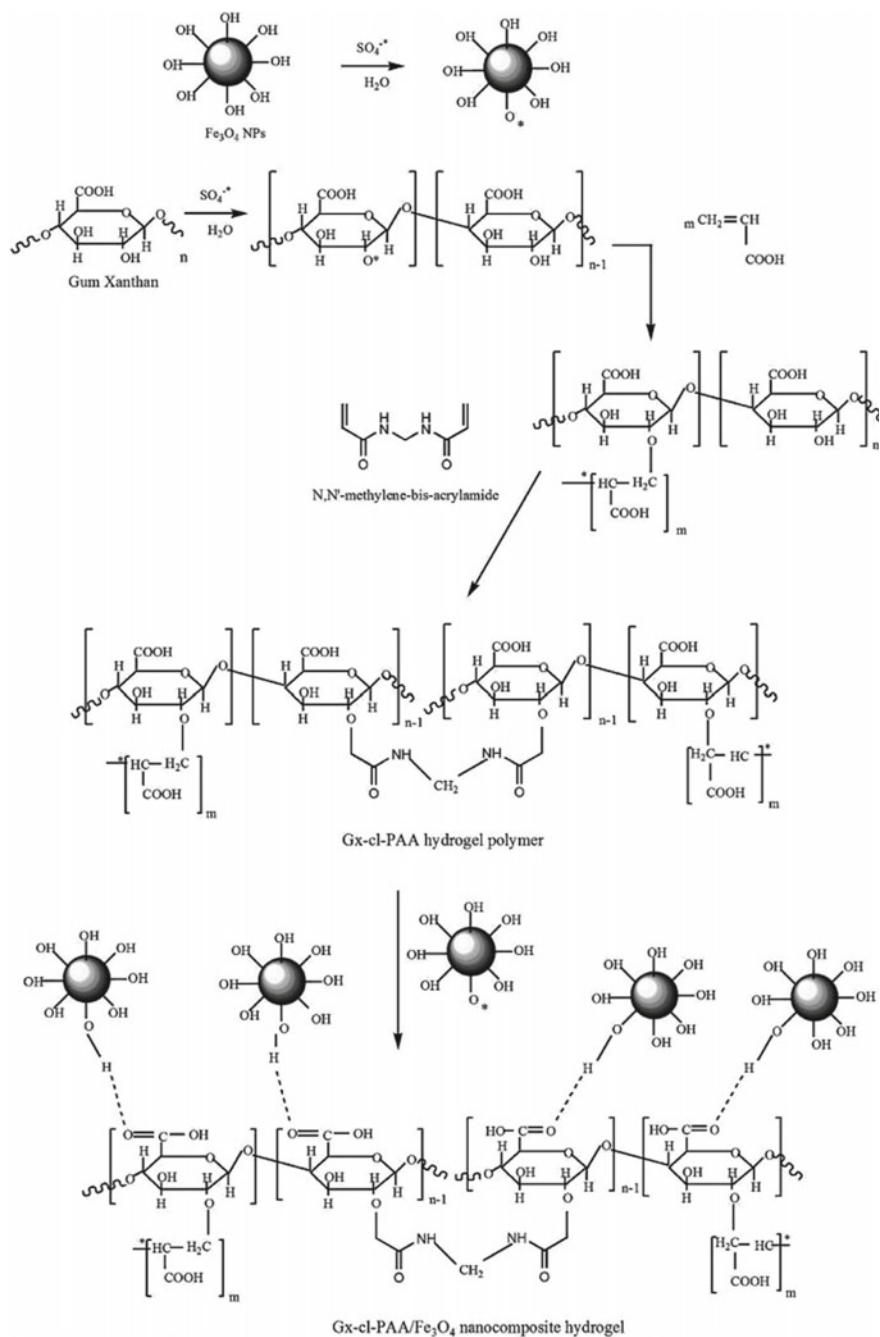


Fig. 2 Proposed mechanism for the synthesis of Fe₃O₄ magnetic nanoparticles based nanocomposite hydrogel [41]

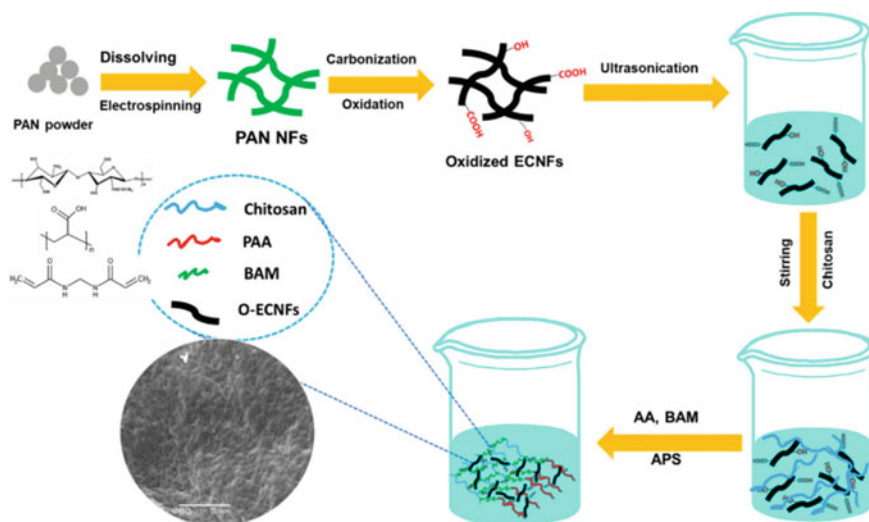


Fig. 3 Illustration for the preparation of hydrogel nanocomposite [60]

5 Factors Affecting the Efficiency of Magnetic-Based Biocomposites for the Adsorption of Dye

5.1 Physicochemical Properties of Magnetic-Based Biocomposite as Dye Adsorbent

The physicochemical properties exhibited by magnetic-based biocomposite plays a key role in their efficiency. In this regard, the types of functional groups on the surface of the biocomposite determines the kind of interaction that will be involved in the adsorption process. The type of functional group expressed by the biocomposite is also determined by the composition of the composite; some of this may have groups such as amine, carboxyl, ester, hydroxyl and so on. The presence of heteroatoms in the functional groups contributes to nonbonding electrons that may promote the interaction required to remove the dyes from the solution. However, these functional groups may be modified in order to improve the efficiency of magnetic-based biocomposite towards the dyes. The surface and porosity of magnetic-based biocomposite play an important role in sorption capacity expressed towards dyes. The larger the active surface area available for adsorption, the better the efficiency expressed towards the dyes. The distribution of pore in the structure of magnetic-based biocomposite is also important as they can trap dye molecules during the sorption process. The more and better distributed the pores are, the better the sorption process for dye removal.

The hydrophilicity of biocomposite is essential. The better the hydrophilic property, the better they interact with dye in solution for removal. Magnetic-based biocomposite with polar functional groups exhibits better hydrophilicity, thus better wettability which reduces the repulsive forces between the surface of the biocomposite and the dye molecules in solution. The nature of dye in solution has a vital role to play in the adsorption process. The molecular size, functional groups and molecular structure of the dyes play important role as well during such interaction. The charge on the surface of the dyes when ionized in solution is important as this determines the kind of interaction that will promote its removal from solution; while some dyes are neutral, some are cationic or anionic.

6 Effect of Operating Parameters on the Sorption of Dyes by Magnetic-Based Biocomposite

Several operation parameters are known to affect the performance of magnetic-based biocomposite towards removing dyes in solution. These parameters include initial dye concentration, temperature, contact time, solution pH and adsorbent dosage.

Efficiency exhibited by magnetic-based biocomposite depends on the interaction between the initial concentrations of dye in solution and the available sorption site on the surface of magnetic-based biocomposite. Previous studies have shown that the adsorption capacity of magnetic-based biocomposite increases as the initial concentration of dye in the solution increase [54]. It has become apparent that the high initial dye concentration promotes high mass transfer driving force for the sorption process [22].

The rate of a chemical reaction can be greatly influenced by temperature; therefore, temperature plays a significant role in understanding whether the sorption process is exothermic or endothermic. The adsorption process is considered to be endothermic if the adsorption capacity increases with an increase in temperature [55]. For the endothermic process, the interaction between the surface of magnetic-based biocomposite and the dyes becomes stronger with an increase in mobility of the dyes as temperature increases. However, if the adsorption capacity increases with a decrease in temperature, the process is considered to be exothermic. Therefore, temperature is a vital contributing factor in understanding the sorption process.

The effect of contact time helps in ascertaining the optimum time required for the dyes to completely occupy the active site for adsorption at the surface of the magnetic-based biocomposite. It may also relate to the time it takes to remove the dye in solution completely. Studies have shown that adsorption capacity and percentage removal improves with time [1–3]. The process is known to increase until equilibrium is attained; at equilibrium, it becomes steady; however, if allowed for long, desorption of dye from the surface of the biocomposite may set in.

Due to the vital impact of pH value on the ionization degree of functional groups, pH is considered to play an important role in understanding the mechanism and

efficiency of adsorption. In most cases, a change in pH value brings about a change in the charges on the surface of magnetic-based biocomposite. The change in charges helps to develop the most suitable conditions for the sorption of dye from solution. A study has shown that the removal efficiency of anionic dyes increase at low pH value while the reverse is the case for cationic dyes [52]. The percentage of removal increases as the adsorbent dose increase while the adsorption capacity reduces. The observation has been related to the fact that as adsorbent dose increases, more active sites become available on the surface of the adsorbent for sorption with the dyes in solution; however, the reduction in adsorption capacity may be attributed to a decrease in the mass transfer of the dye ions from solution to the surface of the adsorbent [7].

7 Desorption

Apart from outstanding performance exhibited by magnetic-based biocomposites, it is much more important that it should have a high regeneration capacity. Therefore, the ability to reuse a biocomposite for a long time before being discarded is vital. The desorption process facilitates the recovery of the dyes in a form that can be re-concentrated and used again. The desorption process further helps to minimize waste generated as the dye adsorbed is recovered without being thrown into the environment. The fact that the dyes may be recovered in a form that can be reused minimizes the process cost. The desorption mode may also aid the understanding of the adsorption process. The desorption process may be achieved using methods that include an acid, organic solvent, base, thermal and mechanical treatments. Some of the acids used include H_2SO_4 , HCl , HNO_3 and H_3PO_4 , while base may be $NaOH$ and liquid NH_3 . The typical organic solvent used may include methanol, acetonitrile, hexane and ethanol.

In most cases, a weak solution of the acid or base is used or a solution of a mixture of acid and organic solvent, depending on the polarity of the adsorbed dye. This may involve agitating the dye-saturated magnetic-based biocomposite with the appropriate solvent to desorb the dye under specified operating conditions. Most desorption or regeneration methods may have shortcomings that can be circumvented; moreover, most studies were conducted at laboratory levels which suggest the need for more studies to be conducted on desorption at a large-scale level.

8 Challenges and Economic Perspective

The economic viability of an adsorbent is essential in its consideration for practical application. However, there is scanty information on the cost evaluation of most reported magnetic-based biocomposites in the literature. Most studies reported laboratory-based experimental studies and not cost implications or large-scale

studies. One major challenge with the practical industrial application of magnetic-based biocomposite is that information on large-scale application is limited, making it difficult to make a detailed comparison with conventional or known adsorbents currently found in the market or in use on a large scale for the removal of dyes in solution. In most cases where low-cost is used to refer to magnetic-based biocomposite, it only meant the initial cost of production at a small scale. However, there is a need to consider and include local availability, transportation, desorption, pretreatment, regeneration cycle and running cost in order to better estimate the actual production cost of magnetic-based biocomposites.

9 Conclusion

This chapter considers the role magnetic-based biocomposite plays in the removal of dyes from solution. It evaluated the preparation, characteristics and application of magnetic-based biocomposite as adsorbents for dye removal in solution. It became evident that magnetic-based biocomposites are potential adsorbents for the removal of dyes in water. However, little information is available on the evaluation and application on a large scale, as most reports have been on laboratory-scale studies. Therefore, there is a need to conduct more studies on the large-scale application of magnetic-based biocomposite as an adsorbent for the removal of dyes in water as well as its economic viability.

References

1. Adewuyi A, Gopfert A, Adewuyi OA, Wolff T (2016) Adsorption of 2-chlorophenol onto the surface of underutilized seed of *Adenopus breviflorus*: A potential means of treating waste water. *J Environ Chem Eng* 4:664–672. <https://doi.org/10.1016/j.jece.2015.12.012>
2. Adewuyi A, Oderinde RA (2019) Chemically modified vermiculite clay: A means to removing emerging contaminant from polluted water system in developing nation. *Polym Bull* 76:4967–4989. <https://doi.org/10.1007/s00289-018-2643-0>
3. Adewuyi A, Oderinde RA (2019) Chemically modified vermiculite clay: a means to remove emerging contaminant from polluted water system in developing nation. *J Polym Bull* 76:4967–4989. <https://doi.org/10.1007/s00289-018-2643-0>
4. Adewuyi A, Yusuf A, Lau WJ, Hojamberdiev M, Oderinde RA (2020) Synthesis of amine imprinted manganese ferrite and its application in the removal of free fatty acid from waste vegetable oil. *Surf Interf* 21:100715. <https://doi.org/10.1016/j.surfin.2020.100715>
5. Akbarzadeh A, Samiei M, Davaran S (2012) Magnetic nanoparticles: preparation, physical properties, and applications in biomedicine. *Nanoscale Res Lett* 7:144. <https://doi.org/10.1186/1556-276X-7-144>
6. Azha SF, Sellaoui L, Engku EHE, Yee CJ, Bonilla- A, Lamine AB, Ismail S (2019) Iron-modified composite adsorbent coating for azo dye removal and its regeneration by photo-Fenton process: synthesis, characterization and adsorption mechanism interpretation. *Chem Eng J* 361:31–40. <https://doi.org/10.1016/j.cej.2018.12.050>

7. Banerjee S, Chattopadhyaya MC (2017) Adsorption characteristics for the removal of a toxic dye tartazine from aqueous solutions by a low cost agricultural by-product. *Arab J Chem* 10:S1629–S1638. <https://doi.org/10.1016/j.arabjc.2013.06.005>
8. Bharathi KS, Ramesh ST (2013) Removal of dyes using agricultural waste as low-cost adsorbents: a review. *Appl Water Sci* 3:773–790. <https://doi.org/10.1007/s13201-013-0117-y>
9. Briao GV, Jahn SL, Foletto EL, Dotto GL (2018) Highly efficient and reusable mesoporous zeolite synthesized from a biopolymer for cationic dyes adsorption. *Colloids Surf A: Physicochem Eng Aspects* 556:43–50. <https://doi.org/10.1016/j.colsurfa.2018.08.019>
10. Carneiro PA, Umbuzeiro GA, Oliveira DP, Zanoni MVB (2010) Assessment of water contamination caused by a mutagenic textile effluent/dyehouse effluent bearing disperse dyes. *J Hazard Mat* 174:694–699. <https://doi.org/10.1016/j.jhazmat.2009.09.106>
11. Chaari I, Fakhfakh E, Medhioub M, Jamoussi F (2019) Comparative study on adsorption of cationic and anionic dyes by smectite rich natural clays. *J Mol Struct* 1179:672–677. <https://doi.org/10.1016/j.molstruc.2018.11.039>
12. Chen W, Chen Y, Huang H, Mahdi Y, Khorram S, Zhao W, Wang D, Qi S, Zhang BJG (2019) Occurrence of *N*-Nitrosamines in the Pearl River delta of China: characterization and evaluation of different sources. *Water Res* 164:114896. <https://doi.org/10.1016/j.watres.2019.114896>
13. Cheng J, Chang PR, Zheng PW, Ma XF (2014) Characterization of magnetic carbon nanotube-cyclodextrin composite and its adsorption of dye. *Ind Eng Chem Res* 53:1415–1421. <https://doi.org/10.1021/ie402658x>
14. Colin N, Maceda-Veiga A, Flor- N, Mora J, Fortuño P, Vieira C, Prat N, Cambra J, de Sostoa A (2016) Ecological impact and recovery of a Mediterranean river after receiving the effluent from a textile dyeing industry. *Ecotoxicol Environ Saf* 132:295–303. <https://doi.org/10.1016/j.ecoenv.2016.06.017>
15. Corrêa GT, de Souza JC, Silva JP, Pividori MI, Zanoni MVB (2020) Determination of temporary dye Basic Red 51 in commercial hair dye, river water and wastewater from hair-dressing salon using graphite-epoxy composite electrode modified with magnetic nanoparticles. *Microchemical J* 159:105485. <https://doi.org/10.1016/j.microc.2020.105485>
16. da Rosa SR, da Rosa BC, Goncalves JO, Pinto LAA, Mallmann ES, Dotto GL (2019) Synthesis of a bio-based polyurethane/chitosan composite foam using ricinoleic acid for the adsorption of Food Red 17 dye. *Int J Biol Macromol* 121:373–380. <https://doi.org/10.1016/j.ijbiomac.2018.09.186>
17. Daengsakul S, Mongkolkachit C, Thomas C, Siri S, Thomas I, Amornkitbamrung V, Maensiri S (2009) A simple thermal decomposition synthesis, magnetic properties, and cytotoxicity of $\text{La}_{0.7}\text{Sr}_{0.3}\text{MnO}_3$ nanoparticles. *Appl Phys A* 96:691–699. <https://doi.org/10.1007/s00339-009-5151-0>
18. de Aragao UG, Freeman HS, Warren SH, Oliveira DP, Terao Y, Watanabe T, Claxton LD (2005) The contribution of azo dyes to the mutagenic activity of the Cristais river. *Chemosphere* 60:55–64. <https://doi.org/10.1016/j.chemosphere.2004.11.100>
19. de Souza JC, da Silva BF, Morales DA, Umbuzeiro GA, Zanoni MVB (2020) Assessment of p-aminophenol oxidation by simulating the process of hair dyeing and occurrence in hair salon wastewater and drinking water from treatment plant. 387:122000. <https://doi.org/10.1016/j.jhazmat.2019.122000>
20. Deng JH, Zhang XR, Zeng GM, Gong JL, Niu QY, Liang J (2013) Simultaneous removal of Cd (II) and ionic dyes from aqueous solution using magnetic graphene oxide nanocomposite as an adsorbent. *Chem Eng J* 226:189–200. <https://doi.org/10.1016/j.cej.2013.04.045>
21. Elkhider KHA, Ihsanullah I, Zubair M, Manzar MS, Mu'azu ND, Al-Harathi MA (2020) Synthesis characterization and dye adsorption performance of strontium ferrite decorated bentonite-CoNiAl magnetic composite. *Arab J Sci Eng* 45:7397–7408. <https://doi.org/10.1007/s13369-020-04544-0>
22. Eren Z, Acar FN (2006) Adsorption of reactive black 5 from an aqueous solution: equilibrium and kinetic studies. *Desalination* 194:1–10. <https://doi.org/10.1016/j.desal.2005.10.022>
23. Gao S, Zhang W, An Z, Kong S, Chen D (2019) Adsorption of anionic dye onto magnetic $\text{Fe}_3\text{O}_4/\text{CeO}_2$ nanocomposite: equilibrium, kinetics, and thermodynamics 37:185–204. <https://doi.org/10.1177/0263617418819164>

24. Habiba U, Siddique TA, Li Lee JJ, Joo TC, Ang BC, Afifi AM (2018) Adsorption study of methyl orange by chitosan/polyvinyl alcohol/zeolite electrospun composite nanofibrous membrane. *Carbohydr Polym* 191:79–85. <https://doi.org/10.1016/j.carbpol.2018.02.081>
25. Hashemian S, Dehghanpor A, Moghahed M (2015) $\text{Cu}_{0.5}\text{Mn}_{0.5}\text{Fe}_2\text{O}_4$ nano spinels as potential sorbent for adsorption of brilliant green. *J Ind Eng Chem* 24:308–314. <https://doi.org/10.1016/j.jiec.2014.10.001>
26. Hassan MM, Carr CM (2018) A critical review on recent advancements of the removal of reactive dyes from dyehouse effluent by ion-exchange adsorbents. *Chemosphere* 209:201–219. <https://doi.org/10.1016/j.chemosphere.2018.06.043>
27. Ito T, Adachi Y, Yamanashi Y, Shimada Y (2016) Long-term natural remediation process in textile dye-polluted river sediment driven by bacterial community changes. *Water Res* 100:458–465. <https://doi.org/10.1016/j.watres.2016.05.050>
28. Kannan N, Rengasamy G (2005) Comparison of cadmium ion adsorption on various activated carbons. *Water Air Soil Pollut* 163:185–201. <https://doi.org/10.1007/s11270-005-0277-y>
29. Khoshsang H, Ghaffarinejad A, Kazemi H, Wang Y, Arandiyan H (2018) One-pot synthesis of S-doped $\text{Fe}_2\text{O}_3/\text{C}$ magnetic nanocomposite as an adsorbent for anionic dye removal: equilibrium and kinetic studies. *J Nanostruct Chem* 8:23–32. <https://doi.org/10.1007/s40097-017-0251-4>
30. Konicki W, Sibera D, Mijowska E, Lenzion-Bielun Z, Narkiewicz U (2013) Equilibrium and kinetic studies on acid dye acid red 88 adsorption by magnetic ZnFe_2O_4 spinel ferrite nanoparticles. *J Colloids Interface Sci* 398:152–160. <https://doi.org/10.1016/j.jcis.2013.02.021>
31. Lellis B, Fávoro-Polonio CZ, Pamphile JA, Polonio JC (2019) Effects of textile dyes on health and the environment and bioremediation potential of living organisms. *Biotechnol Res Innov* 3:275–290. <https://doi.org/10.1016/j.biori.2019.09.001>
32. Li C, Wei Y, Liivat A, Zhub Y, Zhu J (2013) Microwave-solvothermal synthesis of Fe_3O_4 magnetic nanoparticles. *Mater Lett* 107:23–26. <https://doi.org/10.1016/j.matlet.2013.05.117>
33. Li TT, Shu Z, Zhou J, Chen Y, Yu DX, Yuan XM, Wang YX (2015) Template free synthesis of kaolin-based mesoporous silica with improved specific surface area by a novel approach. *Appl Clay Sci* 107:182–187. <https://doi.org/10.1016/j.clay.2015.01.022>
34. Liu J, Li W, Kang X, Zhao F, He M, She Y, Zhou Y (2021) Profiling by HPLC-DAD-MSD reveals a 2500-year history of the use of natural dyes in Northwest China. *Dyes Pigment* 187:109143. <https://doi.org/10.1016/j.dyepig.2021.109143>
35. Ma CM, Hong GB, Wang YK (2020) Performance evaluation and optimization of dyes removal using rice bran-based magnetic composite adsorbent. *Materials* 13:2764. <https://doi.org/10.3390/ma13122764>
36. Mahapatra NN (2016) *Textile dyes*. Woodhead Publishing India Pvt, Boca Raton, CRC Press, New Delhi
37. Makarchuk OV, Dontsova TA, Astrelin IM (2016) Magnetic nanocomposites as efficient sorption materials for removing dyes from aqueous solutions. *Nanoscale Res Lett* 11:161. <https://doi.org/10.1186/s11671-016-1364-2>
38. Malatji N, Makhado E, Ramohlola KE, Modibane KD, Maponya TC, Monama GR, Hato MJ (2020) Synthesis and characterization of magnetic clay-based carboxymethyl cellulose-acrylic acid hydrogel nanocomposite for methylene blue dye removal from aqueous solution. *Environ Sci Pollut Res* 27:44089–44105. <https://doi.org/10.1007/s11356-020-10166-8>
39. Mekkawy HA, Ali MO, El-AM (1998) Toxic effect of synthetic and natural food dyes on renal and hepatic functions in rats. *Toxicol Lett* 95:155–161. [https://doi.org/10.1016/S0378-4274\(98\)80621-8](https://doi.org/10.1016/S0378-4274(98)80621-8)
40. Methneni N, Gonzalez JAM, Loco JV, Anthonissen R, Maele JV, Verschaevae L, Fernandez-Serrano M, Mansour HB (2021) Ecotoxicity profile of heavily contaminated surface water of two rivers in Tunisia. *Environ Toxicol Pharmacol* 82:103550. <https://doi.org/10.1016/j.etap.2020.103550>
41. Mittal H, Kumar V, Saruchi RSS (2016) Adsorption of methyl violet from aqueous solution using gum xanthan/ Fe_3O_4 based nanocomposite hydrogel. *Int J Biol Macromol* 89:1–11. <https://doi.org/10.1016/j.ijbiomac.2016.04.050>

42. Mittal H, Ray S (2016) A study on the adsorption of methylene blue onto gum ghatti/TiO₂ nanoparticles-based hydrogel nanocomposite. *Inter j biol macromol* 88:66–80. <https://doi.org/10.1016/j.ijbiomac.2016.03.032>
43. Mojica Piscioiti ML (2015) Desarrollo de nanopartículas magnéticas para su utilización en el tratamiento médico: Hipertermia. Universidad Nacional de Cuyo
44. Munir M, Nazar MF, Zafar MN, Zubair M, Ashfaq M, Hosseini- A, Khan SUD, Ahmad A (2020) Effective adsorptive removal of methylene blue from water by didodecyldimethylammonium bromide-modified brown clay. *ACS Omega* 5:16711–16721. <https://doi.org/10.1021/acsomega.0c01613>
45. Nejati K, Zabihi R (2012) Preparation and magnetic properties of nano size nickel ferrite particles using hydrothermal method. *Chem Cent J* 6:23
46. Ngulube T, Gumbo JR, Masindi V, Maity A (2017) An update on synthetic dyes adsorption onto clay based minerals: a state-of-art review. *J Environ Manag* 191:35–57. <https://doi.org/10.1016/j.jenvman.2016.12.031>
47. Orts F, del Río AI, Molina J, Bonastre J, Cases F (2018) Electrochemical treatment of real textile wastewater: Trichromy Procion HEXL®. *J Electroanal Chem* 808:387–394. <https://doi.org/10.1016/j.jelechem.2017.06.051>
48. Puri C, Sumana G (2018) Highly effective adsorption of crystal violet dye from contaminated water using graphene oxide intercalated montmorillonite nanocomposite. *Appl Clay Sci* 166:102–112. <https://doi.org/10.1016/j.clay.2018.09.012>
49. Raval NP, Shah PU, Shah NK (2016) Adsorptive amputation of hazardous azo dye congo red from wastewater: a critical review. *Environ Sci Pollut Res* 23:14810–14853. <https://doi.org/10.1007/s11356-016-6970-0>
50. Safarik I, Horska K, Svobodova B, Safarikova M (2012) Magnetically modified spent coffee grounds for dyes removal. *Eur Food Res Technol* 234:345–350. <https://doi.org/10.1007/s00217-011-1641-3>
51. Safarik I, Safarikova M (2010) Magnetic fluid modified peanut husks as an adsorbent for organic dyes removal. *Phys Proc* 9:274–278. <https://doi.org/10.1016/j.phpro.2010.11.061>
52. Salleh MAM, Mahmoud DK, Karim WAWA, Idris A (2011) Cationic and anionic dye adsorption by agricultural solid wastes: a comprehensive review. *Desalination* 280:1–13. <https://doi.org/10.1016/j.desal.2011.07.019>
53. Samadder R, Akter N, Roy AC, Uddin MM, Hossen MJ, Azam MS (2020) Magnetic nanocomposite based on polyacrylic acid and carboxylated cellulose nanocrystal for the removal of cationic dye. *RSC Adv* 10:11945–11956. <https://doi.org/10.1039/D0RA00604A>
54. Santhosh C, Velmurugan V, Jacob G, Jeong SK, Grace AN, Bhatnagar A (2016) Role of nanomaterials in water treatment applications: a review. *Chem Eng J* 306:1116–1137. <https://doi.org/10.1016/j.cej.2016.08.053>
55. Senthilkumaar S, Kalaamani P, Subburaam CV (2006) Liquid phase adsorption of crystal violet onto activated carbons derived from male flowers of coconut tree. *J Hazard Mater* 136:800–808. <https://doi.org/10.1016/j.jhazmat.2006.01.045>
56. Shamraiz U, Hussain RA, Badshah A, Raza B, Saba S (2016) Functional metal sulfides and selenides for the removal of hazardous dyes from Water. *J Photochem Photobiol B* 159:33–41. <https://doi.org/10.1016/j.jphotobiol.2016.03.013>
57. Singamaneni S, Bliznyuk VN, Binek C, Tsybmal EY (2011) Magnetic nanoparticles: recent advances in synthesis, self-assembly and applications. *J Mater Chem* 21:16819–16845. <https://doi.org/10.1039/C1JM11845E>
58. Singh KP, Gupta S, Singh AK, Sinha S (2011) Optimizing adsorption of crystal violet dye from water by magnetic nanocomposite using response surface modeling approach. *J Hazard Mater* 186:1462–1473. <https://doi.org/10.1016/j.jhazmat.2010.12.032>
59. Terdputtakun A, Arqueropanyo O, Sooksamiti P, Janhom S, Naksata W (2017) Adsorption isotherm models and error analysis for single and binary adsorption of Cd(II) and Zn(II) using leonardite as adsorbent. *Environ Earth Sci* 76:777. <https://doi.org/10.1007/s12665-017-7110-y>
60. Thamer BM, Aldalbahi A, Meera MA, El- MH (2020) In situ preparation of novel porous nanocomposite hydrogel as effective adsorbent for the removal of cationic dyes from polluted water. *Polymers* 12:3002. <https://doi.org/10.3390/polym12123002>

61. Wang M, Ma YF, Sun Y, Hong SY, Lee SK, Yoon B, Chen L, Ci LJ, Nam JD, Chen XY, Suhr J (2017) Hierarchical porous chitosan sponges as robust and recyclable adsorbents for anionic dye adsorption. *Sci Rep* 7:18054. <https://doi.org/10.1038/s41598-017-18302-0>
62. Wang PF, Cao MH, Wang C, Ao YH, Hou J, Qian J (2014) Kinetics and thermodynamics of adsorption of methylene blue by a magnetic graphene-carbon nanotube composite. *Appl Surf Sci* 290:116–124. <https://doi.org/10.1016/j.apsusc.2013.11.010>
63. Wang Q, Wang Y, Chen L (2019) A green composite hydrogel based on cellulose and clay as efficient absorbent of colored organic effluent. *Carbohydr Polym* 210:314–321. <https://doi.org/10.1016/j.carbpol.2019.01.080>
64. Wang S, Zhai YY, Gao Q, Luo WJ, Xia H, Zhou CG (2014) Highly efficient removal of acid red 18 from aqueous solution by magnetically retrievable chitosan/carbon nanotube: batch study, isotherms, kinetics, and thermodynamics. *Chem Eng Data* 59:39–51. <https://doi.org/10.1021/je400700c>
65. Wang T, Zhou Y, Cao S, Lu J, Zhou Y (2019) Degradation of sulfanilamide by Fenton-like reaction and optimization using response surface methodology. *Ecotoxicol Environ Saf* 172:334–340. <https://doi.org/10.1016/j.ecoenv.2019.01.106>
66. Wu Q, Feng C, Wang C, Wang Z (2013) A facile one-pot solvothermal method to produce superparamagnetic graphene-Fe₃O₄ nanocomposite and its application in the removal of dye from aqueous solution. *Colloids Surf B: Biointerf* 101:210–214. <https://doi.org/10.1016/j.col surfb.2012.05.036>
67. Wu S, Sun A, Zhai F, Wang J, Xu W, Zhang Q, Volinsky AA (2011) Fe₃O₄ magnetic nanoparticles synthesis from tailings by ultrasonic chemical co-precipitation. *Mat Lett* 65:1882–1884. <https://doi.org/10.1016/j.matlet.2011.03.065>
68. Wu W, He Q, Chen H, Tang J, Nie L (2007) Sonochemical synthesis, structure and magnetic properties of air-stable Fe₃O₄/Au nanoparticles. *Nanotechnol* 18:145609. <https://doi.org/10.1088/0957-4484/18/14/145609>
69. Xia Y, Dai X, Huang S, Tian X, Yang H, Li Y, Liu Y, Zhao M (2013) Fast and highly efficient removal of methylene blue by a novel EDTAD-modified magnetic chitosan material. *Desalin Water Treat* 51:7586–7595. <https://doi.org/10.1080/19443994.2013.777368>
70. Xu J, Yang H, Fu W, Du K, Sui Y, Chen J, Zeng Y, Li M, Zou G (2007) Preparation and magnetic properties of magnetite nanoparticles by sol-gel method. *J Magn Magn Mater* 309:307–311. <https://doi.org/10.1016/j.jmmm.2006.07.037>
71. Xu J, Zhang F, Sun J, Sheng J, Wang F, Sun M (2014) Bio and nanomaterials based on Fe₃O₄. *Molecules* 19:21506–21528. <https://doi.org/10.3390/molecules191221506>
72. Yadav S, Asthana A, Chakraborty R, Jain B, Singh AK, Carabineiro SAC, Susan MABH (2020) Cationic dye removal using novel magnetic/activated charcoal/ β -cyclodextrin/alginate polymer nanocomposite. *Nanomaterials* 10:170. <https://doi.org/10.3390/nano10010170>
73. Yadla SV, Sridevi V, Lakshmi MVVC (2012) A review on adsorption of heavy metals from aqueous solution. *J Chem Biol Phys Sci* 2:1585–1593
74. Yagub MT, Sen TK, Ang HM (2012) Equilibrium, kinetics, and thermodynamics of methylene blue adsorption by pine tree leaves. *Water Air Soil Pollut* 223:5267–5282. <https://doi.org/10.1007/s11270-012-1277-3>
75. Yan H, Li H, Yang H, Li A, Cheng R (2013) Removal of various cationic dyes from aqueous solutions using a kind of fully biodegradable magnetic composite microsphere. *Chem Eng J* 223:402–411. <https://doi.org/10.1016/j.cej.2013.02.113>
76. Yang Y, Yu WY, He SJ, Yu SX, Chen Y, Lu LH, Shu Z, Cui HD, Zhang Y, Jin HY (2019) Rapid adsorption of cationic dye-methylene blue on the modified montmorillonite/graphene oxide composites. *Appl Clay Sci* 168:304–311. <https://doi.org/10.1016/j.clay.2018.11.013>
77. Yao Y, Miao S, Liu S, Ma LP, Sun H, Wang S (2012) Synthesis, characterization, and adsorption properties of magnetic Fe₃O₄@graphene nanocomposite. *Chem Eng J* 184:326–332. <https://doi.org/10.1016/j.cej.2011.12.017>
78. Ying TY, Raman AAA, Bello MM, Buthiyappan A (2020) Magnetic graphene oxide-biomass activated carbon composite for dye removal. *Korean J Chem Eng* 37:2179–2191. <https://doi.org/10.1007/s11814-020-0628-9>

79. Zaini MAA, Cher TY, Zakaria M, Kamaruddin MJ, Setapar SHM, Yunus MAC (2014) Palm oil mill effluent sludge ash as adsorbent for methylene blue dye removal. *Desalination Water Treat* 52:3654–3662. <https://doi.org/10.1080/19443994.2013.854041>
80. Zhang L, Cheng ZJ, Guo X, Jiang XH, Liu R (2014) Process optimization, kinetics and equilibrium of orange G and acid orange 7 adsorptions onto chitosan/surfactant. *J Mol Liq* 197:353–367. <https://doi.org/10.1016/j.molliq.2014.06.007>
81. Zhang YR, Shen SL, Wang SQ, Huang J, Su P, Wang QR, Zhao BX (2014) A dual function magnetic nanomaterial modified with lysine for removal of organic dyes from water solution. *Chem Eng J* 239:250–256. <https://doi.org/10.1016/j.cej.2013.11.022>
82. Zhao YG, Li XP, Yao SS, Zhan PP, Liu JC, Xu CP, Lu YY, Chen XH, Ji MC (2016) Fast throughput determination of 21 allergenic disperse dyes from river water using reusable three-dimensional interconnected magnetic chemically modified graphene oxide followed by liquid chromatography–tandem quadrupole mass spectrometry. *J Chromatogr A* 1431:36–46. <https://doi.org/10.1016/j.chroma.2015.12.089>
83. Zhen G, Muir BW, Moffat BA, Harbour P, Murray KS, Moubaraki B, Suzuki K, Madsen I, Agron-Olshina N, Waddington L, Mulvaney P, Hartley PG (2011) Comparative study of magnetic behavior of spherical and cubic superparamagnetic iron oxide nanoparticles. *J Phys Chem C* 115:327–334. <https://doi.org/10.1021/jp104953z>
84. Zhou Y, Fang X, Wang T, Hu Y, Lu J (2017) Chelating agents enhanced CaO₂ oxidation of bisphenol A catalyzed by Fe³⁺ and reuse of ferric sludge as a source of catalyst. *Chem Eng J* 313:638–645. <https://doi.org/10.1016/j.cej.2016.09.111>